Influence of Annealing on Conduction of High-Density Polyethylene/Carbon Black Composite

Yihu Song, Qiang Zheng

Department of Polymer Science and Engineering, Institute of Polymer Composite, Zhejiang University, Hangzhou 310027, China

Received 2 September 2006; accepted 30 November 2006
DOI 10.1002/app.26076
Published online 2 April 2007 in Wiley InterScience (www.interscience.wiley.com).

ABSTRACT: The high-density polyethylene/carbon black (HDPE/CB) composite with a CB volume fraction of 0.113 is isothermally annealed at various temperatures from 116 to 149°C, covering the positive temperature coefficient (PTC) transition and the negative temperature coefficient regions during heating as well as from 149 to 122°C above the reverse-PTC transition during cooling. Influences of annealing temperature on the resistance–temperature and the resistance–time characteristics are discussed. The results show that both the resistance-temperature and the resistance-time characteristics are highly sensitive to the thermal history. Effects of recrystallization of HDPE and redistribution of CB aggregates in HDPE on the performance are discussed. © 2007 Wiley Periodicals, Inc. J Appl Polym Sci 105: 710–717, 2007

Key words: high-density polyethylene; carbon black-composites; annealing; conduction

INTRODUCTION

Incorporation of conductive particles into a semicrystalline polymer matrix may result not only in conduction but also in a drastic increase in electric resistivity over a temperature range around the melting point (T_m) of the matrix, as is termed as positive temperature coefficient (PTC) effect of resistivity in the literature.[1–5] The strong PTC effect was attributed to the thermal expansion upon melting of the matrix. Such composites with PTC switching effect have found applications in self-regulating heaters, self-resetting overcurrent protectors, solvent sensors, etc., with the advantages of excellent processability, light weight, and flexibility over the conventional inorganic PTC materials.[2] However, the composite shows a negative temperature coefficient (NTC) effect of resistivity at temperatures above T_m due to the redistribution of particles in the melt.[4] It is generally believed that the NTC effect is related to the agglomeration of particles or particle aggregates.[3,5]

The PTC effect strongly depends on the processing condition and thermal history.[6,7] The composites undergoing heating–cooling cycles usually show poor reproducibility of resistivity due to redistribution of particles in the matrix as a result of repeated melting and crystallization.[8,9] Improvement of the reproducibility of resistivity might be achieved through post-heat treatment of the composites.[4,10,11]

In a filled thermoplastic composite, there is always a difference in the interfacial energy between the filler and the matrix, which causes filler particles or aggregates to flocculate during annealing. Annealing of a composite at temperatures below T_m has a complicated influence on crystallinity, crystalline size, and filler distribution and, therefore, on conduction behaviors. Annealing at the solid state might improve crystallinity and enlarge the crystal size of the semicrystalline matrix,[12] which might be critical for enhancement of both stability and long-term service life, with balanced performance of reduced room-temperature resistivity and improved PTC intensity.[11,13] The crystalline structure has obvious influence on the dispersion and on the formation of agglomerates of CB particles. Long-time thermal annealing at elevated temperatures above T_m might cause intermolecular crosslinking,[14] chain scission, and branching,[15] depending on chemical structure of the matrix, which further influence crystal structure in the semicrystalline state.[16] The PTC performance might be deteriorated as thermal oxidative degradation proceeds and crystallinity decreases.[17,18]

Annealing at temperatures below and above T_m has different influences on the redispersion of filler particles in the matrix and also on the PTC/NTC behavior of the composite.[19] Annealing effects are usually investigated in relation to variations in room-temperature resistance, PTC intensity, and resistance–temperature characteristics. The thermal history has a

Correspondence to: Y. Song (s_yh0411@zju.edu.cn).

complicated influence on the resistance–temperature characteristic, while its effect on the time-dependent evolution of conduction is rarely reported. In this article, we shall study the influence of thermal annealing on the conduction behavior of high-density polyethylene (HDPE)/carbon black (CB) composite. For clarifying the effect of thermal history on the time dependence of resistance at given temperatures, we design three sets of experiment where annealing is performed at temperatures located at below and above T_m, respectively, after heating, or above the crystallization temperature (T_c) of HDPE after cooling the melt. Another experiment with a three-stage combined annealing is used to enhance the structural inhomogeneity of the percolation network. Effect of annealing on the resistance–temperature characteristic will also be discussed. To avoid thermal oxidation, all the experiments were performed at temperatures below 149°C.[20]

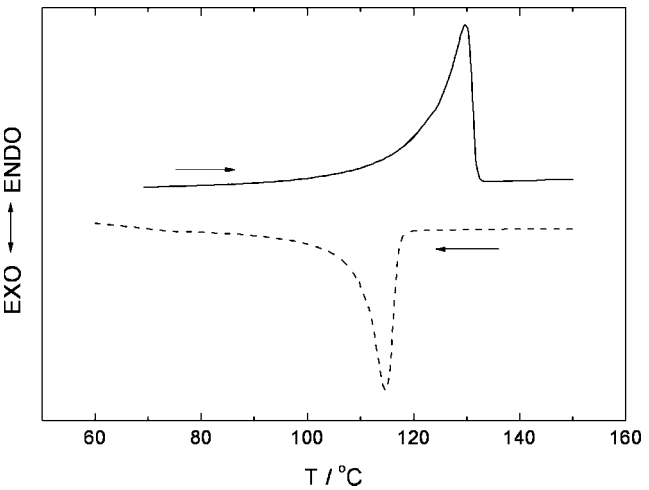

Figure 1 DSC curves of the virgin HDPE/CB composite during heating and cooling.

EXPERIMENTAL

Materials

High-density polyethylene (HDPE, density 0.942 g cm^{-3}, melting index 0.14 g 10 min^{-1}) and acetylene carbon black (CB, particle size 42 nm, Brunauer–Emmett–Teller special surface area 63 m^2 g^{-1}, dibutyl phthalate absorption 1.70 cm^3 g^{-1}) were obtained from Yangzi Ethylene (China) and Shanghai Jishan Chemical (China), respectively. HDPE and CB were mixed on a two-roll mill at 160 ± 5°C for 20 min and then compressed at 165 ± 5°C under 14.7 MPa for 10 min to form sheet samples with a size of 20 mm × 20 mm × 3 mm. The volume fraction of CB was 0.113 above the percolation threshold of 0.080. Two pieces of copper nets were mounted on the opposite wide surfaces of the sheet to ensure good electrical contact with the attached copper electrodes. As described in our earlier articles,[21–23] copper net tightly adhered to the sample surface allowed us to measure the resistance using the simple two-probe measurement, and the contact resistance can be controlled to be as small as possible even after several heating–cooling cycles in the PTC and NTC regions.

Method

Differential scanning calorimetry (DSC) measurement was performed using a Perkin–Elmer series 7 DSC, with a heating/cooling rate of 10°C min^{-1} under dry nitrogen atmosphere. The first run data were analyzed to evaluate the melting and the crystallization behavior of HDPE. Crystallinity of HDPE in the virgin composite was calculated using heat of fusion 287.9 J g^{-1} for perfect polyethylene crystal.[24] Figure 1 shows the DSC curves of the virgin composite during heating and cooling. T_m, T_c, and crystallinity of HDPE are determined as 130°C, 115°C, and 0.58, respectively.

The sheet samples were suspended in air atmosphere in an oven without contact with the wall. The temperature was controlled using the oven, with an accuracy of ±0.5°C. Two-probe resistance measurement was carried out using a M890B$^+$ digital multimeter (Shenzhen Huayi Mastech, China) for measuring resistance.

From technical point of view, the bulk temperature of the sample should be measured for evaluating the resistance–temperature relationship. However, heating at a constant rate resulted in a temperature distribution field inside the sample; that is, the temperature was the highest in the surface and decreased toward the center. Owing to experimental difficulties in evaluating the temperature distribution, the surface temperature of the sample was monitored using a copper–constantan thermocouple attached onto the wide surface of the sample and was recorded using a TM902C digital thermometer (Hongyan Electron, China). Two insulating tapes were used to bind the thermocouple for ensuring close contact with the sample surface. The resistance–temperature curves were measured under a heating/cooling rate of 1°C min^{-1}.

On the basis of DSC measurement and resistance–temperature curves of the virgin sample, four sets of isothermal annealing experiment in air atmosphere were performed. Treatment A was done at temperatures located in the PTC transition region yet below T_m, after heating the sample from room temperature. Treatment B was done at temperatures located in the NTC region (above T_m), after heating the sample from room temperature. Treatment C was done at temperatures above T_c, after cooling the sample from

149°C. A combined annealing was done at three different temperatures during a heating–cooling cycle. The sample was annealed at 122°C after heating from room temperature, at 149°C after heating from 122°C, and at 122°C after cooling from 149°C. The annealing was performed for 72 h at each prescribed temperatures. Resistance as a function of temperature and time during heating/cooling and annealing was recorded.

DSC heating curves of the annealed samples were measured using the procedure same as described earlier.

RESULTS AND DISCUSSION

Resistance–temperature characteristic

As shown in Figure 2, annealing at different temperatures has significantly different influences on the resistance–temperature characteristic of the composite. Treatment A makes resistance during cooling to be considerably higher than that during heating [Fig. 2(a)]. After annealing in the melt, the sample shows an abrupt resistance decrease from 122 ± 1°C to 110°C during cooling [Fig. 2(b,c)], indicating occurrence of a reverse-PTC transition. In Figure 2(d), the sample subjected to combined annealing does not exhibit the reverse-PTC transition, while resistance below 122°C decreases very slightly as the decreasing temperature.

Figure 3 shows the resistance–temperature characteristics of the samples before and after annealing under various conditions. After experienced treatments A, B, and C, the samples exhibit obvious PTC/NTC effect during heating and reverse-PTC effect during cooling. Annealing makes room-temperature resistance to increase by about 1 order of magnitude followed by a slight change in PTC intensity. After the sample is subjected to combined annealing, on the other hand, the room-temperature resistance increases by 2.8 orders of magnitude, and the PTC, the NTC, and reverse-PTC transitions do not take place anymore during thermal cycles.

Figure 4 shows DSC curves of the four annealed samples, and Table I summarizes T_m and the overall crystallinity. The sample after treatment at 149°C

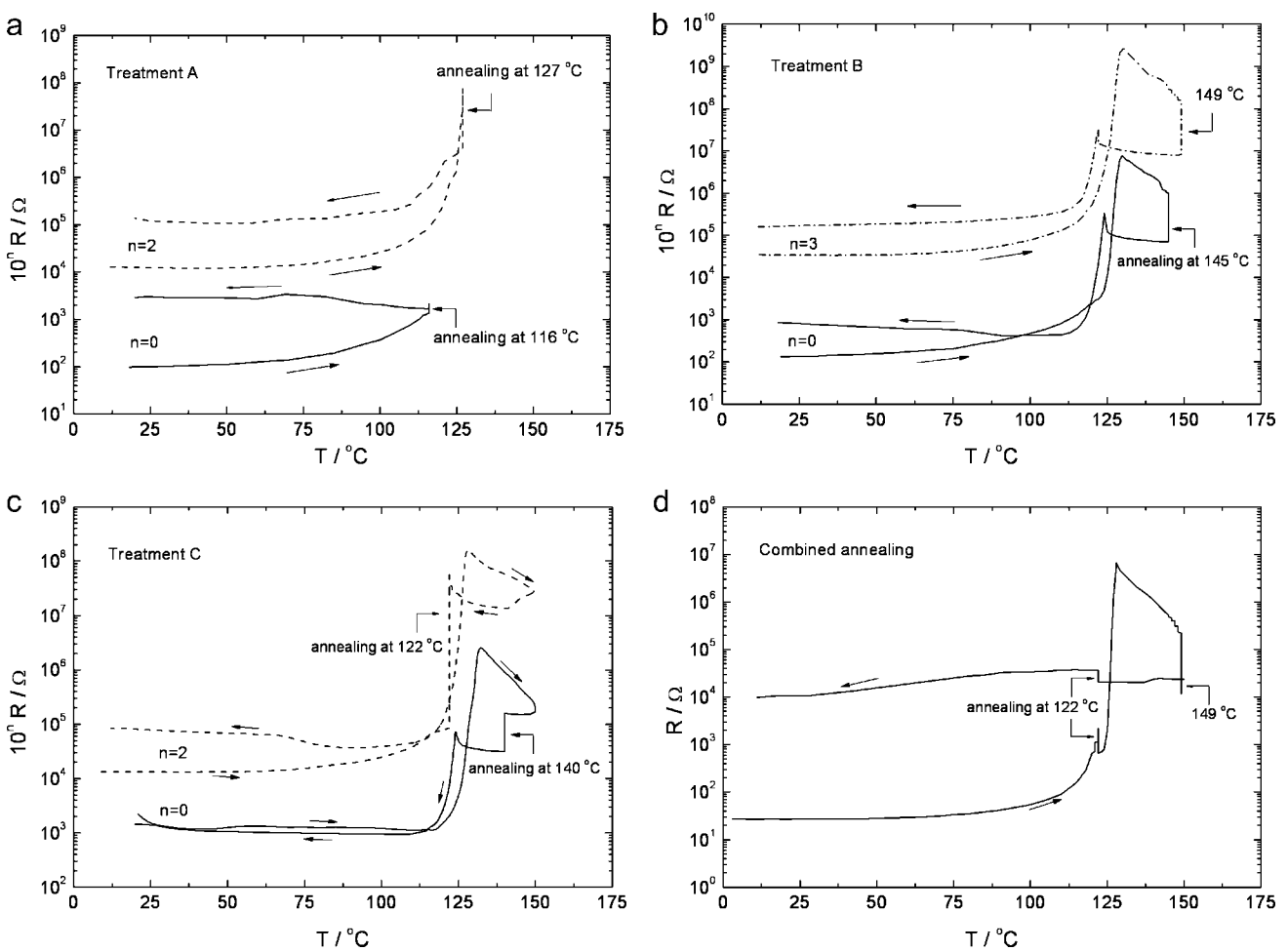

Figure 2 Resistance–temperature characteristic of HDPE/CB composite. The dashed curves in parts (a), (b) and (c) were shifted along the vertical axis by a factor of 10^n for help of view.

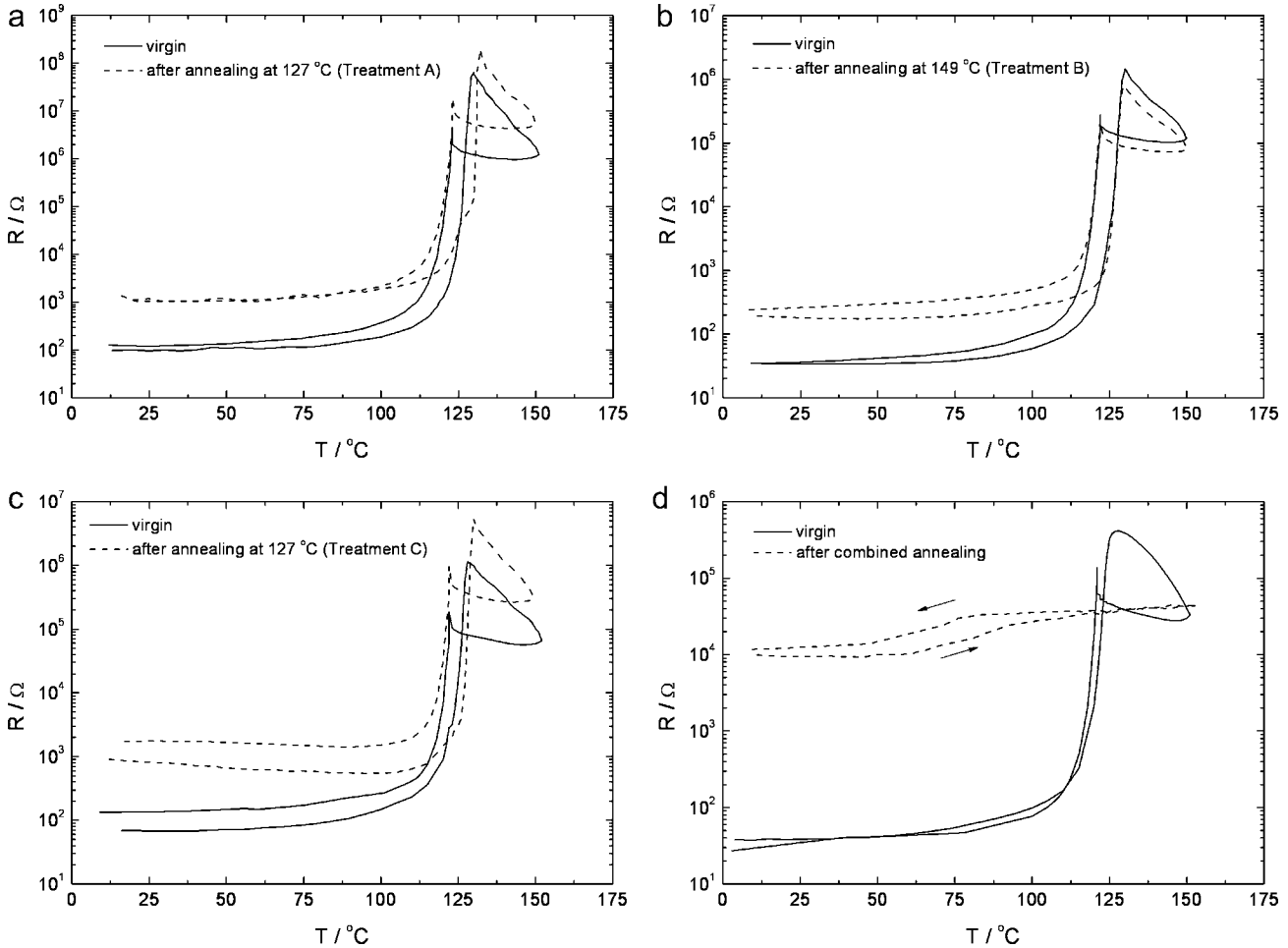

Figure 3 Resistance–temperature characteristic of HDPE/CB composite before (solid curve) and after (dashed curve) annealing.

shows a single melting peak centered at 129.7°C, which is the same as the virgin sample. Furthermore, there is no difference in crystallinity in these two samples. It is clear that annealing in the melt does not influence the crystal structure formed upon cooling from the annealing temperature. On the other hand, the samples annealed at 127°C in treatment A or at 122°C in treatment C exhibit another small peak at 120.8 and 123.2°C, respectively. Annealing in the semicrystalline state allows the molecular diffusion in forming crystals with higher stability, thus, making the major melting peak and the overall crystallinity to increase by 1.7°C and 3%, respectively. The change in crystal structure can be ascribed to lamellar rearrangement.[25] The molecular segregation accompanying with lamellar thickening gives rise to

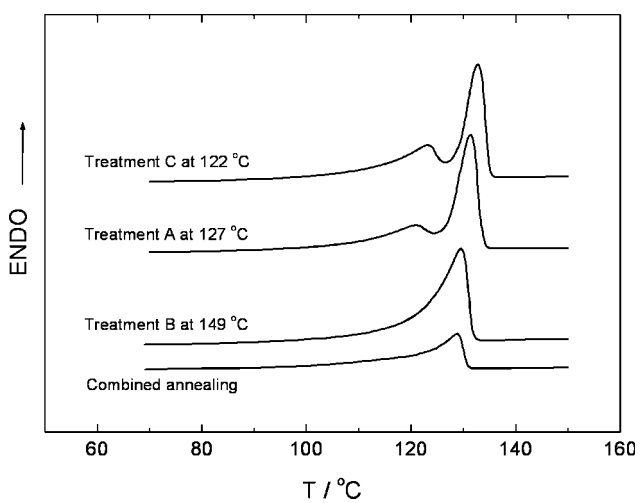

Figure 4 DSC heating curves for the HDPE/CB composite annealed at four conditions as indicated.

TABLE I
Melting Behavior of HDPE in HDPE/CB Composite Annealed at Various Conditions

Sample	T_m (°C)		Crystallinity
Virgin	129.9		0.58
Treatment A at 127°C	131.6	120.8	0.61
Treatment B at 149°C	129.7		0.59
Treatment C at 122°C	133.0	123.2	0.62
Combined annealing	128.8		0.30

the appearance of the low-temperature melting peak. The effect of annealing at 122°C in treatment C comes from crystallization into crystal, with high stability and high order of degree. In comparison with the virgin sample, annealing makes the major melting temperature and the overall crystallinity to increase by 3.1°C and 4%, respectively. Annealing at elevated temperatures usually cause an increase of room-temperature resistance in comparison with the virgin sample, as shown in Figure 2, which could not be explained only from the variation in crystallinity, but is rather related to the redistribution of CB aggregates in the solidified HDPE. The PTC/NTC transition temperature in Figure 3 is exclusively located in the close vicinity of T_m of the main melting peak. The high degree of crystallinity is the reason for the strong PTC transition in Figure 3(a–c).

The combined annealing results in a significant decrease in crystallinity from 58% to 30% in the matrix, and the melting temperature is lowered by 1°C in comparison with the virgin composite (Table I). The combined annealing causes a distinct increase in room-temperature resistance [Fig. 2(d)] and the sample loses the resistance switching characteristic [Fig. 3(d)]. Such changes in conduction behavior is mainly related to a high degree of agglomeration of CB aggregates and to the volume dilution effect due to the increase of the volume fraction of the amorphous phase in HDPE. On the other hand, crosslinking of the matrix is likely to occur under the combined annealing with time as long as 9 days, which results in a small change in density as the material undergoes further thermal treatment.

Resistance relaxation during annealing

Resistance as a function of time at constant temperatures is shown in Figure 5. When the samples were annealed at temperatures located in the PTC transition region, as shown in Figure 5(a,d), resistance increases first and then decreases. The time at the resistance maximum is 1600, 18, and 8 min at temperatures of 116, 122, and 127°C. The rate of resistance decay becomes faster as the annealing temperature is increased. Hou et al.,[26] found that annealing of the CB/ethylene–vinyl acetate copolymer/low-density

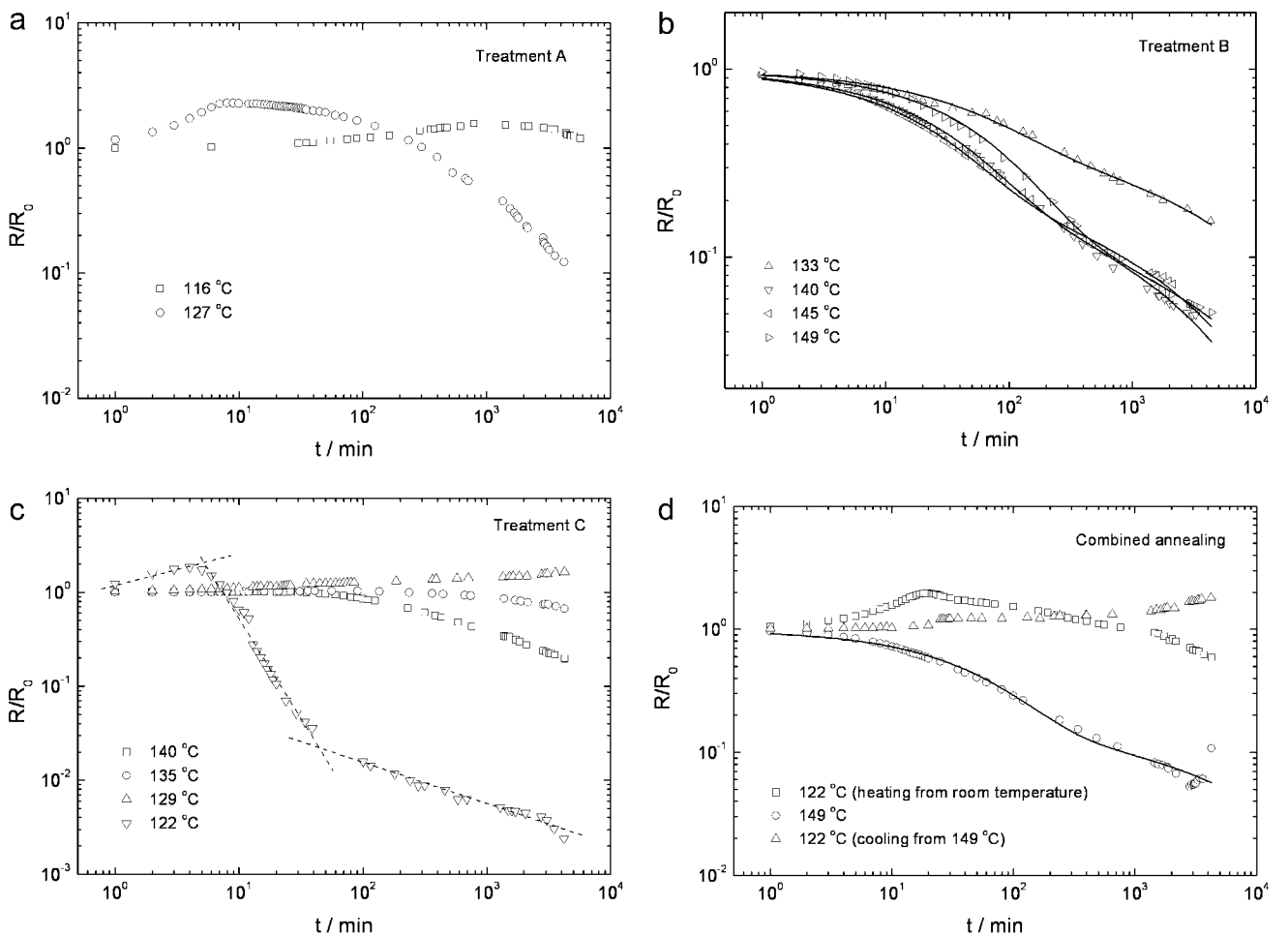

Figure 5 Relative resistance as a function of time. The solid curves in parts (b) and (d) are calculated according to eq. (1) and the dashed lines in part (c) are for guide of the eyes.

polyethylene composites in the PTC transition region causes room-temperature resistance to increase first and then decrease to equilibrium values, dependent on the annealing temperature. However, resistance hardly reaches equilibrium during the annealing process.

The resistance variation during annealing in the PTC transition region involves mainly in the redistribution of CB aggregates due to the melting–recrystallization of the matrix. The recrystallization facilitates the CB aggregates to flocculate in the matrix to produce larger secondary structures, often denoted as agglomerates, so as to decrease superfluous surface energy,[27] which influences the conduction significantly.[28] When the CB/HDPE composite is annealed at temperatures in the PTC transition region, the melting transition (as shown in Fig. 1) makes crystals of low stability to undergo melting and possibly recrystallization. Partial melting of HDPE crystals first leads to the short-distance migration of the adjacent particles, which causes the local breakdown of the conductive clusters and explains the resistance rise in Figure 5(a,d). On the other hand, CB aggregates tend to form clusters in the amorphous phase as recrystallization proceeds, which should result in the resistance decay.

When the samples were heated to temperatures located at the NTC region, as shown in Figure 5(b,d), annealing makes resistance to decrease continuously. This behavior comes from the evolution of the percolation network due to the redistribution of CB aggregates in the melt with a sufficiently reduced viscosity.[29–31] The diffusion of CB aggregates gives rise to the time-dependent resistance.[32,33]

It may be recalled that the relaxation function $f(t)$ for many physical processes is almost universally given by the Kohlrausch–Williams–Watts (KWW) stretched exponential function $f(t) \sim \exp[-(t/\tau)^p]$ (Ref. 34), in which the distribution of relaxation rate depends on sizes of relaxing units.[35] Here p is a measure of the width of the distribution of relaxation times, with $0 \leq p \leq 1$. In colloid science, p is related to fractal dimension D by $p = D/(D + 1)$ (Ref. 36). The KWW relation is suitable for thermally activated processes in a huge variety of complex systems, including polymers, colloids, and glasses. Jund et al.,[37] showed that random walks on percolation clusters in curved spaces accurately results in a KWW-type of relaxation directly connected to the fractal nature of clusters.

We found that a combination of two KWW relations with different relaxation times, τ_1 and τ_2, and exponents, p_1 and p_2, like

$$R/R_0 = \phi \exp[-(t/\tau_1)^{p1}] + (1 - \phi) \exp[-(t/\tau_2)^{p2}] \quad (1)$$

TABLE II
Parameters in Eq. 1 for Describing the Resistance Relaxation at Temperatures Located in the NTC Region

Temperature (°C)	ϕ	τ_1 (min)	τ_2 (min)
133[a]	0.5	60	2500
140[a]	0.7	30	500
145[a]	0.7	23	650
149[a]	0.8	60	1500
149[b]	0.8	45	2800

[a] From Treatment A.
[b] From the combined annealing.

could describe relative resistance R/R_0 as a function of t in almost the entire time scale investigated. Here, ϕ is an adjustment parameter. Equation 1 was applied to fit the measured data using the trial-and-error method, until the calculated curve became considerably close to the measured data. The fitting was further improved by slight adjustment of the five parameters (ϕ, p_1, p_2, τ_1, and τ_2), until the standard deviation was the smallest for each set of data. The fitted curves can well map the measured data with a standard deviation of 0.020–0.024, as shown in Figure 5(b,d) as solid curves. The exponents are estimated as $p_1 = 0.65$ and $p_2 = 0.35$ independent of annealing temperature. The other parameters are shown in Table II. Equation 1 suggests that the resistance relaxation in the NTC region is related to two processes of the percolation network at different length scales. Though the physical meaning of p_2 is ambiguous, the estimated value of p_1 gives a fractal dimension of 1.86, being consistent with that of 1.8–1.9 found in CB/ethylene butylacrylate compolymer or CB/ethylene–propylene–diene terpolymer composites.[27] This fractal dimension value suggests that the fast process with a relaxation time of 20–60 min is due to the formation and growth of CB agglomerates according to the diffusion-limited cluster aggregation mechanism.[38] The slow one with a relaxation time of 500–2800 min might be due to the coarsening of CB agglomerates. Contributions from the two processes are comparable with each other at temperatures slightly above the PTC/NTC transition point. With increasing annealing temperature, contribution from the first process increases while that from the second one decreases.

The resistance relaxation in treatment C [Fig. 5(c)] is quite different from that in treatment B [Fig. 5(b)]. During annealing at 149 and 135°C, resistance predominantly increases at the earlier stage but turns to decrease at the late stage. During annealing at 129°C, the linear increase of resistance in a double-logarithm plot persists in the whole time scale of experiment. It means that annealing at temperatures well above the reverse-PTC transition temper-

ature also introduces two competing processes, i.e., breakdown and reformation of percolation clusters. A higher temperature annealing facilitates the reformation of clusters. A peculiar result is observed during annealing at 122°C, where the reverse-PTC transition due to onset of crystallization exclusively occurs when the composite is cooled from the melt. The resistance–time curve could be divided into three stages. Resistance increases in the first stage before onset of isothermal crystallization of HDPE, which is a behavior reminiscent of resistance relaxation in the melt. In the second stage from 5 to 40 min, the primary crystallization of HDPE gives rise to an increase in the content of the amorphous phase where CB aggregates reside in.[26,39] As the crystallization proceeds, the volume fraction of CB aggregates in the amorphous phase increases, and the gap between CB aggregates becomes narrower. Therefore, the crystallization of HDPE promotes the formation of continuous conductive pathways that build up the percolation network in the amorphous phase. Formation of the percolation network results in an almost linear resistance decay by about 2 orders of magnitude. In the third stage where the secondary crystallization of HDPE occurs, resistance also decreases linearly with time, but the slope is considerably smaller than that in the second stage.

In combined annealing experiment, annealing of 72 h in the PTC transition region (122°C) only causes a slight structural rearrangement in the percolation network [Fig. 5(d)]. Further heating of the sample gives rise to a resistance jump of 4.4 orders of magnitude due to the breakdown of the percolation network at the close vicinity of T_m [Fig. 2(d)]. The melting of HDPE, thus, eliminates the influence of annealing at temperatures below T_m on the distribution of CB particle in the molten matrix. The followed annealing at 149°C makes CB aggregates to agglomerate together with coarsening of CB agglomerates; that is, the distribution of particles becomes very inhomogeneous. This behavior is the same as the single annealing at temperatures in the NTC region. When the sample was cooled down to 122°C, the as-formed conducting pathways are partially broken down during the crystallization of HDPE. Therefore, the resistance–time curve is completely different from that in Figure 5(c) at the same temperature for the sample cooled from 149°C. It means that the agglomeration of CB aggregates in the melt has a significantly marked effect on the time-dependent resistance at temperatures above T_c.

The results show that the time-dependent resistance variation is highly dependent upon the thermal history of HDPE/CB composites. Measurement of the time-dependent resistance during thermal annealing is helpful for investigating the evolution of conduction property and for optimizing the annealing conditions to improve the PTC performance.

CONCLUSIONS

The resistance–temperature characteristic during thermal cycle and the resistance–time characteristic during isothermal annealing are highly dependent on the thermal history for HDPE/CB composite. Annealing at temperatures below T_m or above T_c induces resistance to increase first and then to decrease, reflecting the breakdown and the reformation of percolation network, respectively. During annealing above T_m, the resistance decay occurs exclusively due to the agglomeration of CB aggregates and the formation of percolation network.

References

1. Meyer, J. Polym Eng Sci 1973, 13, 462.
2. Narkis, M.; Ram, A.; Flashmer, F. Polym Eng Sci 1978, 18, 649.
3. Bueche, F. J Appl Phys 1973, 44, 532.
4. Meyer, J. Polym Eng Sci 1974, 13, 706.
5. Narkis, M.; Vaxman, A. J Appl Polym Sci 1984, 29, 1369.
6. Zhang, C.; Yi, X. S.; Asai, S.; Sumita, M. J Mater Sci 2000, 35, 673.
7. Potschke, P.; Fornes, T. D.; Paul, D. R. Polymer 2002, 43, 3247.
8. Asai, S.; Sakata, K.; Sumita, M.; Miyasaka, K. Polym J 1992, 24, 415.
9. Hou, Y. H.; Zhang, M. Q.; Rong, M. Z. Polym Compos 2004, 25, 270.
10. Zhang, M.; Jia, W.; Chen, X. J Appl Polym Sci 1996, 62, 743.
11. Hou, Y.; Zhang, M.; Rong, M.; Yu, G.; Zeng, H. J Appl Polym Sci 2002, 84, 2768.
12. Luo, Y.; Wang, G.; Zhang, B.; Zhang, Z. Eur Polym J 1998, 34, 1221.
13. Huang, Z. Z.; Yue, R.; Chan, H. L. W.; Choy, C. L. Polym Compos 1998, 6, 781.
14. Gugumus, F. Polym Degrad Stab 2002, 76, 329.
15. Gedde, U. W.; Jansson, J.-F. Polym Test 1980, 1, 303.
16. Sun, Y.; Fan, L.; Watkins, K.; Peak, J.; Wong, C. P. J Appl Polym Sci 2004, 93, 513.
17. Han, S. O.; Lee, D. W.; Han, O. H. Polym Degrad Stab 1999, 63, 237.
18. Andreucetti, N. A.; Sarmoria, C.; Curzio, O. A.; Valles, E. M. Radiat Phys Chem 1998, 52, 177.
19. Park, J. S.; Kang, P. H.; Nho, Y. C.; Suh, D. H. J Appl Polym Sci 2003, 89, 2316.
20. Foster, G. N.; Wasserman, S. H.; Yacka, D. J. Angew Makromol Chem 1997, 252, 11.
21. Song, Y.; Pan, Y.; Zheng, Q.; Yi, X. Y. J Polym Sci Part B: Polym Phys 2000, 38, 1756.
22. Song, Y.; Zheng, Q. Polym Int 2004, 53, 1517.
23. Song, Y.; Zheng, Q.; Yi, X. Y. J Polym Sci Part B: Polym Phys 2004, 42, 1212.
24. Brandrup, J. Polymer Handbook, 3rd ed.; Wiley: New York, 1989.
25. Matsuda, H.; Aoike, T.; Uehara, H.; Yamanobe, T.; Komoto, T. Polymer 2001, 42, 5013.
26. Hou, Y. H.; Zhang, M. Q.; Mai, K. C.; Rong, M. Z.; Yu, G.; Zeng, H. M. J Appl Polym Sci 2001, 80, 1267.
27. Jager, K.-M.; McQueen, D. H. Polymer 2001, 42, 9575.

28. Miyasaka, K.; Watanabe, K.; Jojima, E.; Aida, H.; Sumita, M.; Ishikawa, K. J Mater Sci 1982, 17, 1610.
29. Kang, P. H.; Nho, Y. C. J. Ind Eng Chem 2001, 7, 199.
30. Tang, H.; Liu, Z. Y.; Piao, J. H.; Chen, X. F.; Lou, Y. Z.; Li, S. H. J Appl Polym Sci 1994, 51, 1159.
31. Lee, M. G.; Nho, Y. C. Radiat Phys Chem 2001, 61, 75.
32. Sumita, M.; Takenaka, K.; Asai, S. Compos Interface 1995, 3, 253.
33. Asai, S.; Sumita, M. J Macromol Sci Phys 1995, 334, 283.
34. Campbell, I.; Giovannella, C. Relaxation in Complex Systems and Related Topics; Plenum: New York, 1990.
35. Chamberlin, R. V. Phys Rev Lett 1999, 82, 2520.
36. Martin, J. E. Phys Rev A 1987, 36, 3415.
37. Jund, P.; Jullien, R.; Campbell, I. Phys Rev E 2001, 63, 036131.
38. Mrakin, P. Phys Rev Lett 1983, 51, 1119.
39. Lee, J. C.; Nakajima, K.; Ikehara, T.; Nishi, T. J Appl Polym Sci 1997, 65, 409.